

Conjugate-Root Offset-QAM for Orthogonal Multicarrier Transmission

Maximilian Matthé, Gerhard Fettweis

Abstract—Current implementations of OFDM/OQAM are restricted to band-limited symmetric filters. To circumvent this, non-symmetric conjugate root (CR) filters are proposed for OQAM modulation. The system is applied to Generalized Frequency Division Multiplexing (GFDM) and a method for achieving transmit diversity with OQAM modulation is presented. The proposal reduces implementation complexity compared to existing works and provides a more regular phase space. GFDM/CR-OQAM outperforms conventional GFDM in terms of symbol error rate in fading multipath channels and provides a more localized spectrum compared to conventional OQAM.

Index Terms—Quadrature Amplitude Modulation, Multicarrier Modulation, Space-Time Coding

I. INTRODUCTION

With 5G on the horizon, new waveforms for the PHY layer are investigated that are suitable for the upcoming requirements [1]. In particular, good time-frequency localization (TFL) of the transmit signal is required to cope with asynchronicities [2] and to provide a low out-of-band (OOB) radiation, which is needed for spectral agility and carrier aggregation. Filtered multicarrier (MC) systems [3] provide the means for good TFL by adaptation of the prototype filter and spectral agility is achieved by switching on and off certain subcarriers. High spectral efficiency is important to serve the increased demand for high speed data access [1]. Hence, a future waveform should transmit symbols at the Nyquist rate in order to not waste valuable time-frequency resources.

Even in a distortion-free channel, the Balian-Low theorem (BLT) prohibits the distortion-free reconstruction of complex valued-symbols sent at Nyquist rate when using filters with good TFL [4]. Hence, in terms of symbol error rate (SER), QAM MC systems with good TFL perform worse than orthogonal systems without good TFL. One possibility to circumvent the BLT is to transmit real-valued symbols at twice the Nyquist rate, which was initially proposed in [3]. This gave rise to the well known OFDM/OQAM [5] MC system where both orthogonality and good TFL is kept by using Offset-QAM (OQAM), which is proposed for upcoming 5G networks [1].

In current OQAM proposals, the employed real-valued prototype filter is required to be bandlimited and symmetric and a phase shift of $\frac{\pi}{2}$ is maintained between adjacent subcarriers.

In [6], low-complexity implementations of these schemes are described and also a method is proposed to relax the requirement of symmetry of the employed prototype filter which is advantageous since it is shown in [7], that non-symmetric filters can be more robust against multipath fading. However, the approach presented in [6] suffers from an increased implementation complexity compared to conventional OQAM since it requires to use two poly-phase networks (PPNs).

In this paper we contribute another version of MC OQAM modulation, named conjugate-root (CR) Offset-QAM (CR-OQAM), which allows to use the class of non-symmetric CR filters, removing the $\frac{\pi}{2}$ phase shift and providing means for an easier implementation compared to [6]. We further apply CR-OQAM to GFDM [8], which is another 5G candidate waveform that normally uses QAM modulation and hence suffers from the BLT. With CR-OQAM, we provide a well-localized orthogonal system, improving the SER performance in fading multipath channels compared to standard GFDM. Additionally, time-reversal space-time-coding (TR-STC) [9] is applied to GFDM/CR-OQAM to exploit multi-antenna diversity, showing that in GFDM STC can be combined with OQAM modulation which is a known issue in OFDM/OQAM [10]. In [11], FBMC/COQAM is proposed, being equivalent to GFDM using OQAM. However, compared to the present paper, neither CR-OQAM nor STC is covered therein.

The remainder is organized as follows: Sec. II describes the conventional OQAM transceiver, whereas the proposed modification is presented in Sec. III. Sec. IV describes the application of CR-OQAM to GFDM and performance simulations are provided in Sec. V. Finally, Sec. VI concludes.

II. CONVENTIONAL OFDM/OQAM

In OFDM/OQAM, complex-valued data symbols $c_{k,m}$ are transmitted on K subcarriers, where real and imaginary part are offset by $\frac{T}{2}$ where T is the symbol duration. Each symbol is pulse-shaped with a symmetric, real-valued pulse shaping filter $g(t)$ [3], [5]. The transmission equation is given by

$$x(t) = \sum_{\substack{k=0 \\ m \in \mathbb{Z}}}^{K-1} (c_{k,m}^R g(t - mT) + j c_{k,m}^I g(t - mT - \frac{T}{2})) j^k w^{kt} \quad (1)$$

where $w = \exp(j2\pi F)$, $F = \frac{1}{T}$, and $c_{k,m}^R$ and $c_{k,m}^I$ are real and imaginary part of $c_{k,m}$, respectively. Note that, due to the factor j^k , adjacent subcarriers differ by a phase shift of $\frac{\pi}{2}$.

At the receiver, matched filtering is carried out, i.e.

$$\hat{c}_{k,m}^R = \Re(x(t) j^{-k} w^{-kt} * g(-t))|_{t=mT} \quad (2)$$

$$\hat{c}_{k,m}^I = \Im(x(t) j^{-k} w^{-kt} * g(-t))|_{t=(\frac{1}{2}+m)T}, \quad (3)$$

arXiv:1504.00126v2 [cs.IT] 23 Jun 2015

Manuscript received..., revised
The responsible editor during processing at IEEE WCL was ...
Here goes some more editorial text...
The DOI of this document is ...
This work has been performed in the framework of the FP7 project ICT-619555 RESCUE, which is partly funded by the European Union.
M. Matthé and G. Fettweis are with Vodafone Chair Mobile Communication Systems, Technische Universität Dresden, Germany (e-mail: maximilian.matthe@ifn.et.tu-dresden.de; fettweis@ifn.et.tu-dresden.de)

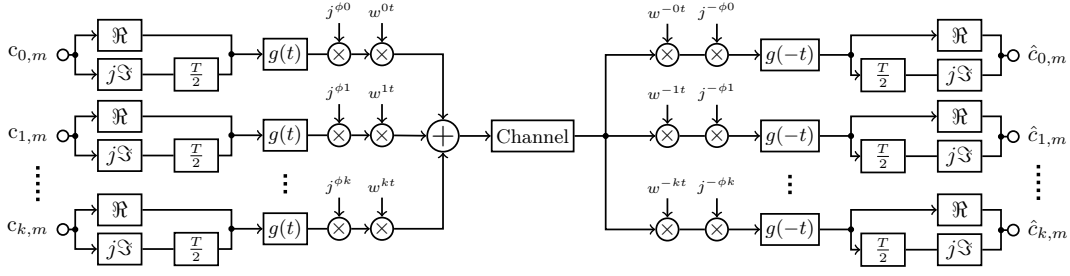


Fig. 1. Block diagram of the OFDM/OQAM ($\phi = 1$) and OFDM/CR-OQAM ($\phi = 0$) transceiver.

where convolution $x(t) * y(t)$ is defined as

$$(x(t) * y(t))|_{t=\tau} = \int_{-\infty}^{\infty} x(t)y(\tau - t)dt. \quad (4)$$

The corresponding block diagram of the OFDM/OQAM transceiver is presented in Fig. 1. For perfect reconstruction, the orthogonality conditions between the k th and $(k + \kappa)$ th subcarrier that are given by [5, eq. (13)]

$$\Re\{(g(t)j^{-\kappa}w^{-\kappa t} * g(-t))|_{t=mT}\} = \delta(\kappa, m) \quad (5)$$

$$\Re\{(jg(t)j^{-\kappa}w^{-\kappa t} * g(-t))|_{t=(\frac{1}{2}+m)T}\} = 0 \quad (6)$$

$$\Im\{(g(t)j^{-\kappa}w^{-\kappa t} * g(-t))|_{t=(\frac{1}{2}+m)T}\} = 0 \quad (7)$$

$$\Im\{(jg(t)j^{-\kappa}w^{-\kappa t} * g(-t))|_{t=mT}\} = \delta(\kappa, m) \quad (8)$$

must be fulfilled for all κ, m . With the relations $\Re\{ja\} = -\Im\{a\}$ and $\Im\{ja\} = \Re\{a\}$, (5) and (6) are equivalent to (8) and (7), respectively. These conditions are in particular fulfilled, when $g(t)$ is a symmetric, half-Nyquist filter with band-limitation $G(f) = 0, |f| \geq F$ [2].

The convolution is expressed with the Fourier transform \mathcal{F} by

$$(g(t)w^{-\kappa t} * g(-t))|_{t=\tau} = \mathcal{F}^{-1}\{S_k(f)\}(\tau) = s_k(\tau), \quad (9)$$

where $S_k(f) = G(f - kF)G^*(f)$ is the spectrum of the intercarrier interference (ICI) from the k' th to the $(k' + k)$ th subcarrier, $s_k(t)$ is the corresponding time domain function, $G(f)$ is the Fourier transform of $g(t)$ and $(\cdot)^*$ denotes complex conjugation. Fig. 2a depicts $s_1(t)$ for a root raised cosine (RRC) filter with roll-off $\alpha = 0.75$.

III. CONJUGATE-ROOT MULTICARRIER OQAM

In literature, mostly symmetric half-Nyquist filters are employed for MC OQAM systems. We propose the application of non-symmetric CR filters [12], [13] for MC OQAM systems.

Assume an even $H(f)$ with band limitation $H(f) = 0$ for $|f| \geq F$. Then, $H(f)$ fulfills the 1st Nyquist criterion [12] iff

$$\forall f \in [0, F] : H(f) + H(f - F) = 1. \quad (10)$$

Its corresponding half-Nyquist filter is given by $G(f) = \sqrt{H(f)}$ where the most prominent example is the symmetric raised cosine (RC) and RRC pair. The according non-symmetric CR filter $G^C(f)$ is constructed by

$$G^C(f) = \begin{cases} H(f) + j\sqrt{(1 - H(f))H(f)} & f \geq 0 \\ H(f) - j\sqrt{(1 - H(f))H(f)} & f < 0 \end{cases} \quad (11)$$

with impulse response $g^C(t) = \mathcal{F}^{-1}\{G^C(f)\}$. Note that both $G^C(f)$ and $G^C(f)(G^C(f))^*$ are Nyquist filters (cf. (10)).

Fig. 2b shows the RRC and CRRC filter response. The ICI $S_1^C(f)$ between adjacent subcarriers with CR filters equals

$$S_1(f) = \sqrt{H(f)H(f - F)} \quad (12)$$

$$S_1^C(f) = G^C(f - F)[G^C(f)]^* \quad (13)$$

$$= jS_1(f), \quad (14)$$

where (14) follows from (11) and (10). Therefore, since

$$s_1^C(t) = js_1(t), \quad (15)$$

the real and imaginary part of the ICI are exchanged when using a CR filter compared to its standard half-Nyquist version. Both $S_1^C(f)$ and $s_1^C(t)$ are presented in Fig. 2c.

Hence, if $g(t)$ fulfills (5)–(8), the according $g^C(t)$ fulfills

$$\Re\{(g^C(t)w^{-\kappa t} * g^C(-t))|_{t=mT}\} = \delta(\kappa, m) \quad (16)$$

$$\Re\{(jg^C(t)w^{-\kappa t} * g^C(-t))|_{t=(\frac{1}{2}+m)T}\} = 0. \quad (17)$$

Note, that compared to (5)–(8) the factor j^k has been removed. Consequently, an OFDM/CR-OQAM system that uses a CR filter $g^C(t)$ can be described by the modulation equation

$$x(t) = \sum_{\substack{k=0 \\ m \in \mathbb{Z}}}^{K-1} (c_{k,m}^R g^C(t - mT) + jc_{k,m}^I g^C(t - mT - \frac{T}{2}))w^{kt}, \quad (18)$$

the demodulation equations

$$\hat{c}_{k,m}^R = \Re(x(t)w^{-\kappa t} * g^C(-t))|_{t=mT} \quad (19)$$

$$\hat{c}_{k,m}^I = \Im(x(t)w^{-\kappa t} * g^C(-t))|_{t=(\frac{1}{2}+m)T} \quad (20)$$

and the block diagram in Fig. 1 with $\phi = 0$.

The time-frequency phase space for OFDM/OQAM and OFDM/CR-OQAM is shown in Fig. 3a where real and imaginary values are depicted with \circ and \bullet , respectively. Due to the missing $\frac{\pi}{2}$ phase shift between subcarriers, the grid is more regular for the CR-OQAM case. Hence, OFDM/CR-OQAM can be seen as two parallel OFDM/PAM systems transmitting with a time offset of $\frac{T}{2}$ and a phase shift of $\frac{\pi}{2}$. The more regular phase space can lead to simpler equalization and pilot design and theoretic analysis might be easier to accomplish.

In [6] conjugate OFDM/OQAM is proposed, where forward-time and time-reversed transmit and receive filters alternate along the subcarriers, which is clearly different compared to the present proposal. Using this approach, the

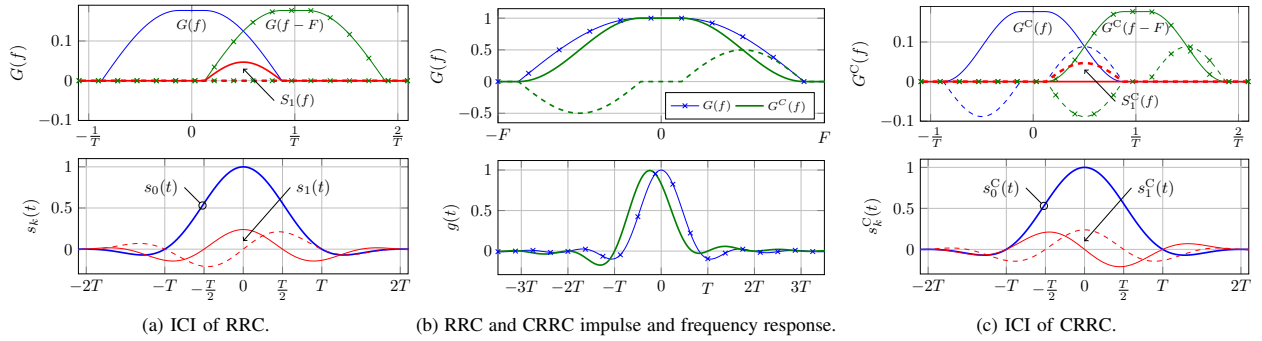


Fig. 2. Solid and dashed lines represent real and imaginary part, respectively. (a), (c) ICI of adjacent channel. (b) Filter response of RRC and CRRC filters.

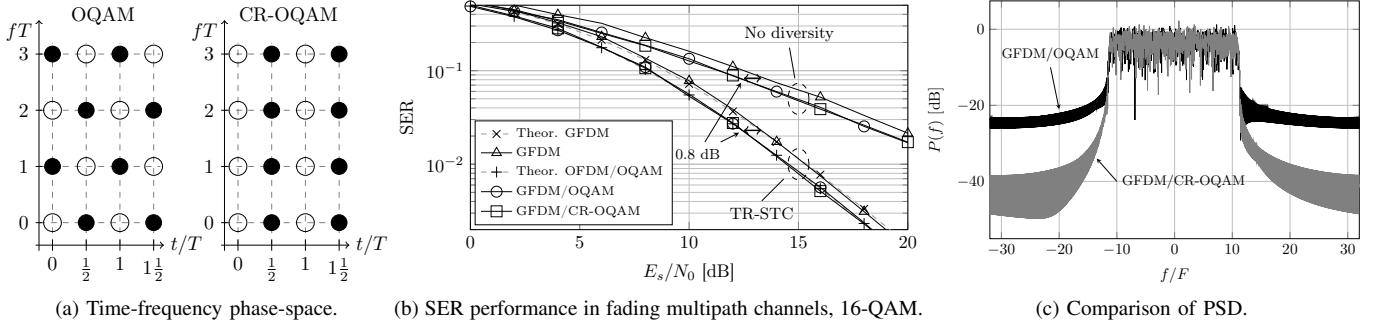


Fig. 3. Time-frequency phase space and performance comparison of OQAM and CR-OQAM.

symmetry requirement of the prototype filters is relaxed, but still a phase shift between subcarriers is kept, hence keeping the phase space equal to conventional OQAM. Also in [6], low-complexity formulations for conventional and conjugate OQAM are given. It is stated that due to the use of alternating filters for conjugate OQAM, the system requires two PPNs for implementation, which increases the complexity. In the present approach, the symmetry requirement is relaxed by using CR filters and changing the transmit phase space. Since only one prototype filter type is used, only one PPN is required, leading to the same implementation complexity as conventional OQAM in [6]. However, in [6] the use of one $N/2$ -point complex DFT per symbol is required, which would be changed to one N -point real DFT per symbol due to the changed phase space for OFDM/CR-OQAM implementations.

IV. APPLICATION OF CR-OQAM IN GFDM

OFDM/OQAM is a streaming based, filtered MC system, where every symbol overlaps with its adjacent symbols in time. GFDM [8] is a filtered MC system, where circular convolution is applied instead of linear. Hence, its transmit signal exhibits a block structure and subsequent blocks can be decoupled by a cyclic prefix (CP) to ease equalization.

GFDM is modeled in discrete base band with sampling period T_s . The transmit signal \vec{x} is given by

$$\vec{x} = \mathbf{A}\vec{d}, \quad (21)$$

where the columns of the matrix \mathbf{A} contain circular time-frequency shifted versions of a prototype transmit filter $g[n]$ with distance KT_s in time and $1/(KT_s)$ in frequency, where

K is the number of subcarriers. \vec{d} contains the complex-valued data symbols to be transmitted with the block. By appending a CP, frequency domain channel equalization can be carried out at the receiver, yielding the signal \hat{x} and zero-forcing (ZF) or matched filter (MF) detection is applied

$$\hat{d}_{ZF} = \mathbf{A}^{-1}\hat{x} \quad \hat{d}_{MF} = \mathbf{A}^H\hat{x}, \quad (22)$$

where $(\cdot)^H$ denotes Hermitian conjugate. A main property of GFDM is its good TFL of the transmit filter, which allows to achieve a low OOB radiation and robustness against asynchronicity [8]. However, when using QAM modulation, the BLT prohibits orthogonality completely, which impacts MF performance while ZF detectors introduce noise-enhancement and only exist for certain parameter configurations [14]. Hence, with perfect synchronization, SER performance of GFDM is worse compared to an orthogonal system.

To circumvent this problem, OQAM modulation can be applied, which provides orthogonality but still keeps the advantageous property of good time-frequency localization. Looking at the phase space of CR-OQAM (Fig. 3a), the GFDM/CR-OQAM modulator is given by

$$\vec{x} = \mathbf{A}\Re\{\vec{d}\} + j\mathcal{C}_{\frac{K}{2}}(\mathbf{A}\Im\{\vec{d}\}), \quad (23)$$

where $\mathcal{C}_u(\cdot)$ denotes a circular rotation of its argument by u elements. At the receiver, the CR-OQAM detection with the matched filter is simply achieved by

$$\Re\{\hat{d}\} = \Re\{\mathbf{A}^H\vec{x}\}, \quad \Im\{\hat{d}\} = \Im\{\mathbf{A}^H\mathcal{C}_{-\frac{K}{2}}(\vec{x})\}. \quad (24)$$

Time-reversal space-time coding (TR-STC) [15] can be applied to GFDM/CR-OQAM to provide transmit diversity in a

TABLE I
GFDM SIMULATION PARAMETERS

Parameter	Symbol	QAM	OQAM	CR-OQAM
Subsymbol spacing	K	64	64	64
Subsymbol count	M	7	7	7
Filter	$g[n]$	RC	RRC	CRRC
Filter rolloff	α	0.5	1	1
Detector		ZF	MF	MF

fading multipath environment. TR-STC was initially developed for single-carrier systems, where two subsequent time domain codewords are decoupled by a CP and jointly space-time encoded. For GFDM, one block is treated as a single-carrier codeword and the TR-STC is applied onto two subsequent GFDM blocks [9]. At the receiver, both GFDM blocks are recovered by the TR-STC and processed by the GFDM detector. The approach can be applied to both GFDM and GFDM/(CR-)OQAM, but GFDM/(CR-)OQAM is expected to outperform conventional GFDM due to the kept orthogonality.

V. PERFORMANCE EVALUATION

The SER performance of GFDM and GFDM/(CR-)OQAM with and without TR-STC has been evaluated in Rayleigh fading multipath channels. The power delay profile of the channel between the transmit and receive antennas is modelled with length 16 where the tap powers decay linearly in log scale from 0dB to -16dB. The GFDM parameters are given in Tab. I and the simulation results are presented in Fig. 3b, where perfect channel state information was available at the receiver. The theoretic equations for GFDM/QAM are taken from [9]. Note that as GFDM/(CR-)OQAM is orthogonal it performs equal to OFDM/OQAM and corresponding equations are also taken from [9, eq. (19)] with noise-enhancement $\xi = 1$.

GFDM/OQAM outperforms conventional GFDM with and without TR-STC due to the orthogonality introduced by the OQAM modulation. The performance gap equals the noise-enhancement of GFDM, which is 0.8 dB in the presented configuration. Both GFDM and GFDM/(CR-)OQAM show a diversity gain of 2 when combined with TR-STC.

Since in the present configuration, OQAM and CR-OQAM both use the same equalization scheme, the benefits of non-symmetric filters proposed in [7] cannot be shown in the SER curve. Fig. 3c shows the comparison of the power spectral density (PSD) of GFDM/OQAM and GFDM/CR-OQAM using one guard symbol (GS) [8], where the application of CRRC filters significantly reduces OOB emission. As shown in [8], high OOB emission is mainly due to abrupt signal changes at the boundaries of the GFDM block. By using GSs with QAM modulation and ISI-free filters, these discontinuities are avoided. However, due to the half-symbol shift when using OQAM with RRC filters, employing GSs does not remove signal discontinuities. On the other hand, as CRRC filters have zeros at twice the symbol rate, application of GS efficiently reduces OOB emission, making the use of CR-OQAM advantageous over that of conventional OQAM.

VI. CONCLUSION

This paper has presented an alternative approach for the implementation of Offset-QAM when using non-symmetric conjugate root filters. With the proposal, no phase shift between subcarriers is required, making the CR-OQAM time-frequency phase space more regular and compared to existing work, implementation complexity is reduced. Orthogonality conditions have been stated for the OFDM/CR-OQAM system and it was proven that CR filters fulfill these. CR-OQAM has been applied to GFDM to create an orthogonal system with good TFL. Space-time code aiming for transmit diversity was applied to GFDM/(CR-)OQAM and, outperforming the conventional space-time coded GFDM system. GS were efficiently employed to reduce OOB emission when using CR filters, which is not possible with conventional OQAM.

REFERENCES

- [1] G. Wunder, P. Jung, M. Kasparick, T. Wild, F. Schaich, Y. Chen, S. Brink, I. Gaspar, N. Michailow, A. Festag, L. Mendes, N. Cassiau, D. Ktenas, M. Dryjanski, S. Pietrzyk, B. Eged, P. Vago, and F. Wiedmann, "SGNOW: non-orthogonal, asynchronous waveforms for future mobile applications," *IEEE Communications Magazine*, vol. 52, no. 2, pp. 97–105, Feb. 2014.
- [2] B. Le Floch, M. Alard, and C. Berrou, "Coded orthogonal frequency division multiplex [TV broadcasting]," *Proceedings of the IEEE*, vol. 83, no. 6, pp. 982–996, Jun. 1995.
- [3] R. W. Chang, "Synthesis of Band-Limited Orthogonal Signals for Multichannel Data Transmission," *The Bell Systems Technical Journal*, vol. 45, no. 10, pp. 1775–1796, 1966.
- [4] J. J. Benedetto, C. Heil, and D. F. Walnut, "Gabor Systems and the Balian-Low Theorem," in *Gabor Analysis and Algorithms*, H. G. Feichtinger and T. Strohmer, Eds. Birkhäuser, 1998, ch. 2, pp. 85–122.
- [5] P. Siohan, C. Siclet, and N. Lacaille, "Analysis and design of OFDM/OQAM systems based on filterbank theory," *Signal Processing, IEEE Transactions on*, vol. 50, no. 5, pp. 1170–1183, May 2002.
- [6] L. Vangelista and N. Laurenti, "Efficient implementations and alternative architectures for OFDM-OQAM systems," *IEEE Transactions on Communications*, vol. 49, no. 4, pp. 664–675, Apr. 2001.
- [7] K. Feher, "An asymmetrical pulse shaping technique to combat delay spread," *IEEE Transactions on Vehicular Technology*, vol. 42, no. 4, pp. 425–433, 1993.
- [8] N. Michailow, M. Matthé, I. Gaspar, A. Navarro Caldevilla, L. L. Mendes, A. Festag, and G. Fettweis, "Generalized Frequency Division Multiplexing for 5th Generation Cellular Networks," *IEEE Transactions on Communications*, vol. 62, no. 9, pp. 3045–3061, 2014.
- [9] M. Matthe, L. L. Mendes, I. Gaspar, N. Michailow, D. Zhang, and G. Fettweis, "Multi-user time-reversal STC-GFDMA for future wireless networks," *EURASIP Journal on Wireless Communications and Networking*, vol. 2015, no. 1, p. 132, May 2015.
- [10] C. Lélé, P. Siohan, and R. Legouable, "The Alamouti Scheme with CDMA-OFDM/OQAM," *EURASIP Journal on Advances in Signal Processing*, vol. 2010, no. 1, pp. 1–14, Jan. 2010.
- [11] H. Lin and P. Siohan, "Multi-carrier modulation analysis and WCP-COQAM proposal," *EURASIP Journal on Advances in Signal Processing*, vol. 2014, no. 1, p. 79, 2014.
- [12] T. Demechai, "Pulse-shaping filters with ISI-free matched and unmatched filter properties," *IEEE Transactions on Communications*, vol. 46, no. 8, p. 992, 1998.
- [13] C. Tan and N. Beaulieu, "Transmission Properties of Conjugate-Root Pulses," *IEEE Transactions on Communications*, vol. 52, no. 4, pp. 553–558, Apr. 2004.
- [14] M. Matthé, L. L. Mendes, and G. Fettweis, "GFDM in a Gabor Transform Setting," *IEEE Communications Letters*, vol. 18, no. 8, pp. 1379–1382, 2014.
- [15] N. Al-Dhahir, "Single-carrier frequency-domain equalization for space-time block-coded transmissions over frequency-selective fading channels," *IEEE Communications Letters*, vol. 5, no. 7, pp. 304–306, Jul. 2001.